Send Orders for Reprints to reprints@benthamscience.ae

Open Access

Experimental and Numerical Investigation on Bending Capacity of Steel-concrete Composite Truss Girder

Wang Yang[1,2*] and Li Tian[2]

[1]*School of Civil Engineering, Taizhou Vocational & Technical College, Taizhou, Zhejiang 318000, P.R. China;* [2]*School of Civil Engineering, Zhengzhou University, Zhengzhou, Henan 450002, P.R. China*

Abstract: This article presents an experimental investigation on the bending capacity of steel-concrete composite truss girder (SCCTG). Four full-scale specimens named CB1, CB2a, CB2b and CB3 respectively, are tested and numerical analyzed. Stress distribution, load-displacement relationship, load-slip relationship and ultimate bending capacity of SCCTGs are investigated. The results show that SCCTG follows plane section assumption on the whole. SCCTG has a higher ultimate bearing capacity and good performance of deformation. Concrete slab and the steel truss can work together better using denser studs. In elastic stage, the effective width of the SCCTG flange plate remains the same with negligible variation. While in plastic stage, the effective width increases. Tests also prove that there is obvious shear lag effect in the concrete compression flange. Three-dimensional numerical model by finite element package ABAQUS is established to examine the bending behaviour of SCCTG. Hopefully, an acceptable correlation has been observed between the analytical and experimental results. There is obvious shear lag effect in the concrete compression flange. Shear lag should be paid great attention when designing and calculating the bearing capacity and deformation of SCCTG.

Keywords: Bending behavior, effective width, experimental study, shear lag, steel-concrete composite truss girder (SCCTG).

1. INTRODUCTION

Compared with ordinary composite beam, steel-concrete composite truss girder (SCCTG) is recognized as an original kind of composite beam [1]. SCCTG is characterized by economic, higher bending rigidity and capacity. This type of SCCTG features steel truss, concrete slab and shear stud. Many scholars have conducted a number of experimental and theoretical researches on this type of composite truss [2-6]. SCCTG exhibits higher stiffness than ordinary composite beam. Ultimate strength can keep constant when dimensions of upper chord member reduced. Tests also indicate that truss members bear majority of the vertical shear force in SCCTG [7]. Slip between upper chord and concrete slab increases gradually from mid-span to support point. And shear studs near the supports bear more horizontal shear force [8]. Additionally, beam deflection will result secondary stresses and further cause buckling of the web members. Thus, web buckling should be considered when determining ultimate strength of SCCTG. Relevant design formulas are put forward based on various experimental researches on shear stud, shrink effect of concrete slab and full-scale bending tests of SCCTG. Those formulas include effective width of composite truss considering parameters such as width-span ratio, span-depth ratio, load pattern, degree of shear connection and thickness of concrete slab [9, 10]. However, this new type of SCCTG has not been given an adequate research effort to understand fully their behavior and rationalize their design. Full-scale SCCTG testing is also needed to verify the analytical solutions to obtain convincing practical design models.

Therefore, four full-scale specimens named CB1, CB2a, CB2b and CB3 respectively, are designed and tested. Stress distribution and failure mode of SCCTGs are investigated. Based on test results, convincing finite element models which can be used in further researches are established.

2. TEST SPECIMENS

2.1. Design and Dimensions

Four full-scale specimens named CB1, CB2a, CB2b and CB3 respectively are included in this research. Specific members and main dimensions are given as Fig. (**1**) and Table **1**. In order to make sure the truss and slab work together without shear studs failure in advance, transverse steel bars of 6mm diameter are lay, at the top and bottom region, each 150mm in the transverse direction of the slab. In the longitudinal direction, steel bars of 6mm diameter are lay, at the top and bottom region, each 200mm in the longitudinal direction of the slab (Fig. **1**). Thus, those transverse and longitudinal steel bars can work as steel bar net.

Shear studs have a dimension of 16mm in diameter and 50mm in height. Stud space is 400mm in specimen CB1 and 100mm in specimen CB2a, CB2b and CB3. Three kinds of steel pipes such as D70-3, D70-6 and D114-8 are used (note that the first number indicates diameter of the pipe and the second number indicates the thickness of the pipe). Gusset plates are welded in all connections of the steel truss. Steel plate which has a dimension of 10mm in thickness and 100mm in width is chosen as upper chord of truss Fig. (**1**).

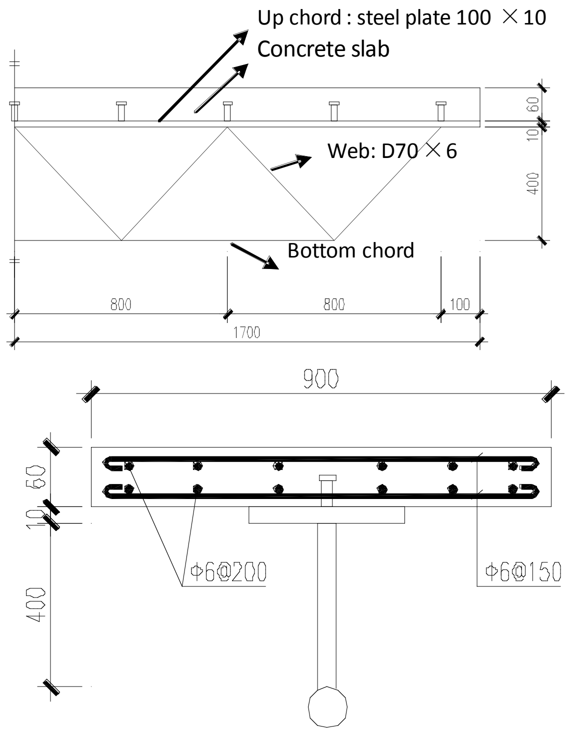

Fig. (1). Detail drawing of SCCTG.

Table 1. Dimensions of SCCTG specimens.

Specimen	Stud (mm) diameter×height@space	Bottom chord A=Area
CB1	Φ16×50@400	D70-3.0 (A=631mm^2)
CB2a	Φ16×50@100	D70-3.0 (A=631mm^2)
CB2b	Φ16×50@100	D70-6.0 (A=1206mm^2)
CB3	Φ16×50@100	D114-8.0（A=2664mm^2）

2.2. Material

Steel bar used in the concrete has yield strength of 275N/mm^2 and ultimate strength of 475 N/mm^2. Steel member used in the truss was Q235 steel with nominal yield stress of 245MPa. Table **2** shows a list of material properties of the steel used in the test, obtained from the coupon tests. Fig. (**2**) shows the processing schematic diagram of SCCTG.

Table 2. Properties of members used in the test.

Type	Yield stress (MPa)	Ultimate stress (MPa)	Elongation rate (%)
Steel bar	275	475	37.7
Steel pipe	245	450	30.2
Shear stud	325	520	26.5

Fig. (2). Processing schematic diagram of SCCTG.

3. LOADING PROGRAM

Fig. (**3**) shows the general arrangement of test specimen. A 500kN actuator was used to produce vertical load below the reaction loading device (Figs. **3**-**5**). The actuator was arranged at the middle of a rigid loading beam in order to achieve a design load distribution ratio of 1:1. By using the rigid loading beam, two points on the specimen are loaded simultaneously in the vertical direction. Note that these two points separate the specimen into three equal parts. Fig. (**5**) shows the loading program used in the test. Both load-control loading program and displacement-control loading program are included in the tests. In the beginning, load-control loading program was conducted. While the deflection or deformation were distinct, displacement-control loading program was used until final failure.

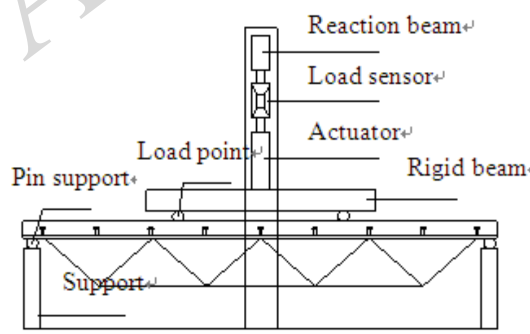

Fig. (3). Load diagram of SCCTG.

Fig. (4). Load diagram in test.

4. MEASUREMENT

Responses of the test specimens were monitored and measured by load cells, displacement transducers, and strain gauges. All data were continuously recorded using a computer data acquisition system. A load cell attached to the head of the actuator measured the vertical load produced by the actuator (Fig. **5**). Three displacement transducers that have a resolution of 0.01 mm were used to measure the deflections between the span. Additional displacement transducers had used to measure displacement and rotations of end supports of the specimen.

Fig. (5). Load reaction frame of SCCTG.

Along the longitudinal direction of the specimen, 3 points were chosen to measure the strain of the slab. For each point, ten strain gauges were glued on the top surface of the slab (Figs. **6** and **7**).

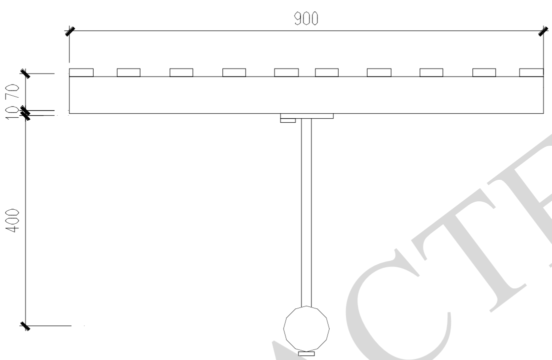

Fig. (6). Strain gauge layout.

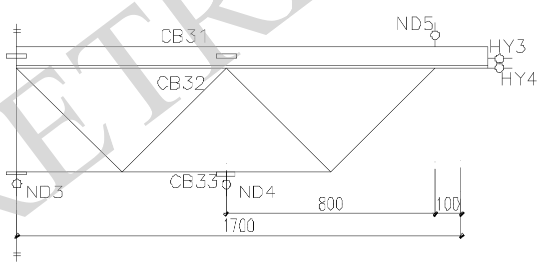

Fig. (7). Displacement measurement.

5. TEST RESULTS

5.1. Damage Evolution

a. Specimen CB1

Fig. (**8**) gives strain gauge layout and load system of specimen CB1. In the initial elastic stage, elongation stress in concrete slab was small. When crack detected, beam deflection reached 6mm which was 1/567 of beam span. As load increasing, bottom chord member yield and notable deformation occurred. Several vertical crack fissures could be observed along the concrete slab. Those fissures inclined toward mid-span and evolved distinct as the load increased, shown in Fig. (**9**). After then, bottom chord yield completely and beam deflection keep increasing. Crush effect was gradually observed in the compressive region of the slab. In final failure mode, fissure in concrete slab reached 10mm at most and compressive slab region crushed seriously (Fig. **10**).

Fig. (8). Strain gauge layout.

Fig. (9). Crack distribution of CB1.

（a）compressive crush

（b）crack at slab bottom

Fig. (10). Damage of concrete slab on CB1.

b. Specimen CB2a, CB2b

Compared with CB1, specimen CB2a is characterized by denser shear studs which produce higher horizontal shear force. In test, steel truss and concrete slab work collaboratively and exhibit good performance with each other. Experiment phenomenon similar to CB1 was observed during the test (Fig. **11**). Difference between specimens CB2b and CB2a is recognized that bottom chord member of CB2b is consist of steel pipe D70-6.0. While bottom chord of CB2a is consist of steel pipe D70-3.0, specimen CB2b exhibits higher bending capacity. Experiment phenomenon of CB2b is similar to CB2a during the test.

Fig. (11). Loading diagram for CB2a.

c. Specimen CB3

Specimen CB3 displays similar performance as CB2a and CB2b. Serious fissure is observed in specimen CB3 at the end of test. Several fissures extend across the height of concrete slab and the slab crushes heavily.

5.2. Comparative Analysis

Strain analysis indicates there is shear lag effect in concrete slab. Maximum strain is monitored at middle of slab. It can be predicted that shear studs within the slab result stress concentration. And shear lag effect aggravates the stress concentration in the slab. Not surprisingly, shear lag effect influences the rigidity and capacity of SCCTG and produces large deformation.

Take specimen CB2b as an example. Fig. (**12**) shows the strain distribution of the composite beam at mid-span point while the beam members are elastic. It can be found that neutral axis lies at the slab middle and almost no slip is observed. Generally, the whole section follows the plane section assumption.

Load-displacement curves are illustrated as Fig. (**13**). In initial of test, relationship between vertical load and deflection keeps linear for members as material stays in elastic stage. With the load increasing, strain measurements indicate stress increases gradually for truss members and slab. Neutral axis moves upward after bottom chord yields and concrete slab cracks due to excessive tensile stress. Load-displacement curves display distinct turning point which demonstrates the test SCCTG shows plastic behavior. In addition, rigidity of SCCTG reduces rapidly after bottom chord yields although bending capacity still keep climbing.

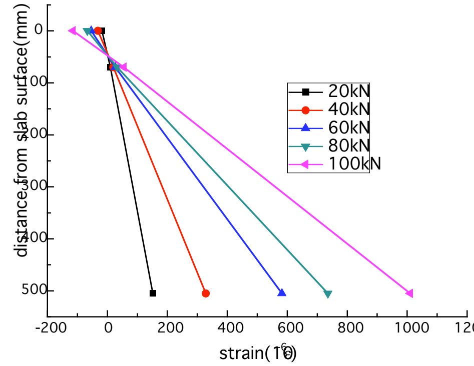

Fig. (12). Strain distribution in the mid-span section for CB2b.

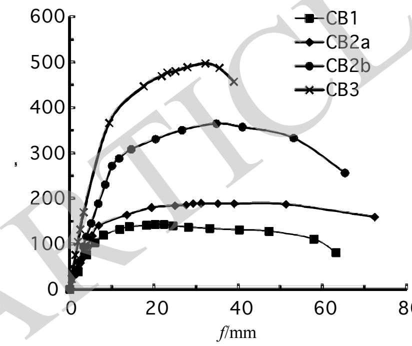

Fig. (13) Load-deformation relationship.

Due to the difference of bottom chord members and shear connecting degree, different beam performances are observed. Comparative analysis show high shear connecting degree can make the composite beam perform well collaboration. Generally, SCCTGs display fine bending and ductile behavior.

6. NUMERICAL SIMULATION

6.1. Finite Element Model

To investigate the bending behaviour of SCCTG, a 3-dimensional numerical model is developed by the finite element package ABAQUS. Fig. (**14**) shows the numerical model. Three dimensional and eight-nodes solid element C3D8R is used to simulate concrete slab. While the steel truss members are simulated by three dimensional beam elements B31 (up chord) and truss element (bottom chord and web member). A special kind of spring connector is used to simulate the nonlinear property of shear studs.

In each numerical model, the loading program is in accordance with the real test, including boundary conditions. The numerical results are compared with the experimental results in order to verify the finite element methods which are used to launch further studies for SCCTG.

6.2. FEM Bending Capacity

Fig. (**15**) shows the contour band of displacement for specimen CB1 using finite element method. Fig. (**16**) shows the comparison of experimental and numerical load-deflection curves of four test specimens. An acceptable correlation has been observed between the analytical and experimental results. In addition, Fig. (**17**) gives the load-slip relationships between stud and slab at the end supports of the beams. Compared with experiments, initial stiffness and bending capacity by numerical models are higher than that by experiments. In numerical models, the yielding, slip and failure of shear studs are simulated by introducing a sharp decrease in the nonlinear load-slip relationship for shear studs. Table **3** shows the comparison of bending capacity.

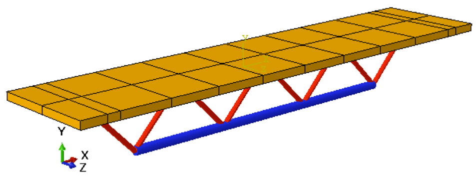

Fig. (14). Finite element model of SCCTG.

However, almost identical initial stiffness is obtained from all the numerical models. This can be observed clearly from the unloading trace which represents the initial elastic stiffness. In specimen CB1, shear connection degree is lower than other specimens as stud spaces are large. As a result, bending capacity reduces rapidly as shear studs yield and fail. In comparison, specimens CB2a, CB2b and CB3 display high bending capacity although some individual studs damage.

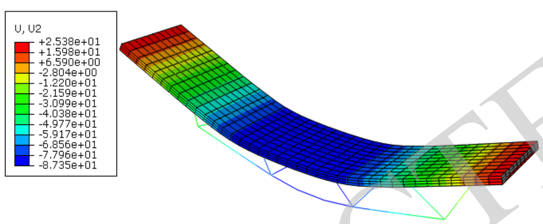

Fig. (15). Displacement contours of CB1.

Table 3. Comparison of bending capacity.

Specimens	FEM P_{u1}(kN)	Experiment P_{u2} (kN)	P_{u1} /P_{u2}
CB1	153.64	143.03	1.07
CB2a	220.86	189.37	1.17
CB2b	394.16	364.80	1.08

6.3. Stress distribution of concrete slab

Stress distribution by numerical model in the middle of concrete slab is provided as Fig. (**18**).

$$b_e = \frac{\int_{-b/2}^{b/2} \sigma_x \mathrm{d}x}{\sigma_{\max}} \quad (1)$$

Distribution of stress along the plate width direction indicates shear lag effect. At each load step, stress in middle of slab is larger than near nodes in width direction. When load reaches elastic limit bearing capacity, effective width of SCCTG can be calculated from stress distributed on concrete slab based on equation (1). Specifically, effective width of the four specimens is 614mm, 622mm, 625mm and 631mm respectively, which indicates almost identical effective width is obtained for CB1, CB2a, CB2b and CB3 during elastic stage. However, when SCCTG members enter into the plastic stage, concrete slab of SCCTG experiences stress plastic redistribution and becomes uniform. And effective width of the four specimens is 678mm, 693mm, 692mm and 698mm respectively. According to Eurocode 4 Design of composite steel and concrete structures, effective width can be calculated by L/4 where L represents the clear span of the composite beam. Considering Eurocode 4, effective width is 800mm which is 16 percent larger than that obtained from

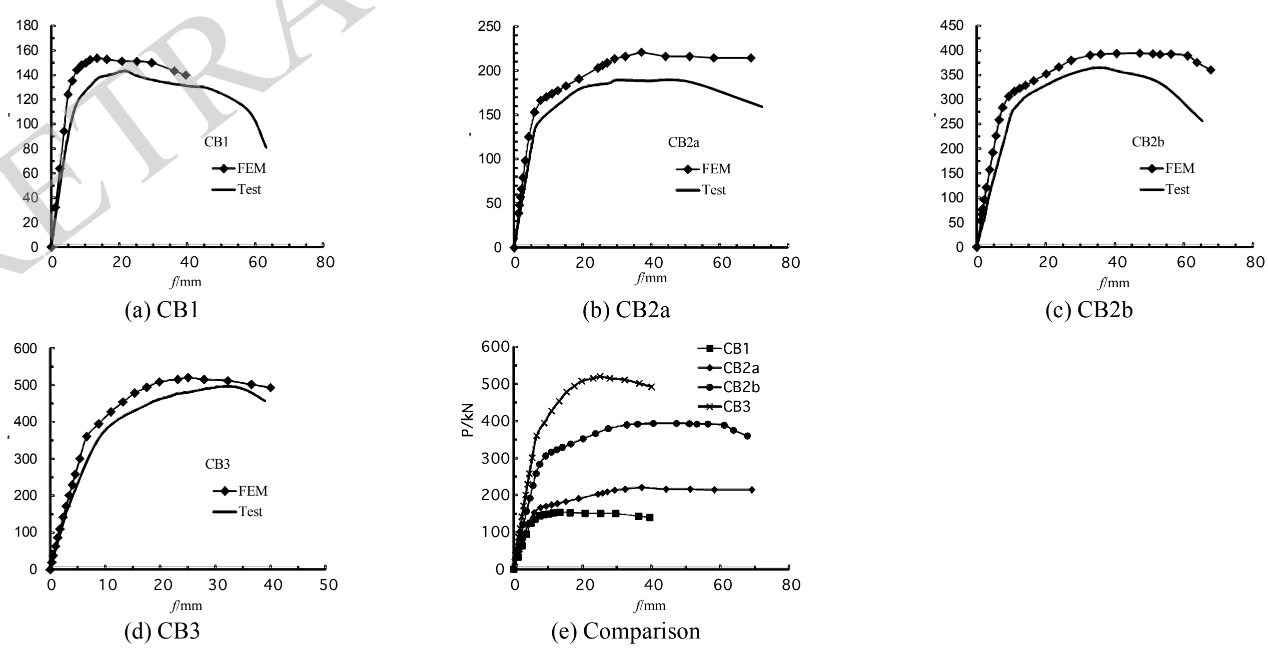

Fig. (16). Load-deflection curves.

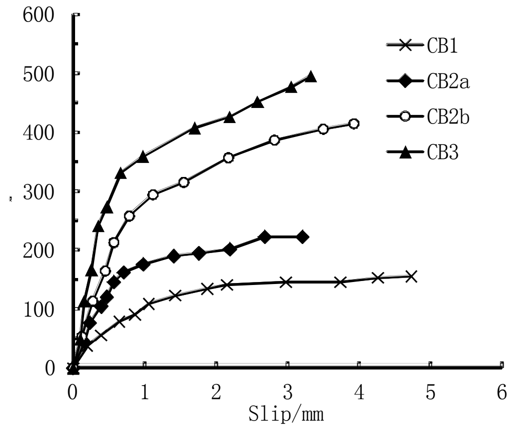

Fig. (17). Relative slip between the concrete slab and the steel slab.

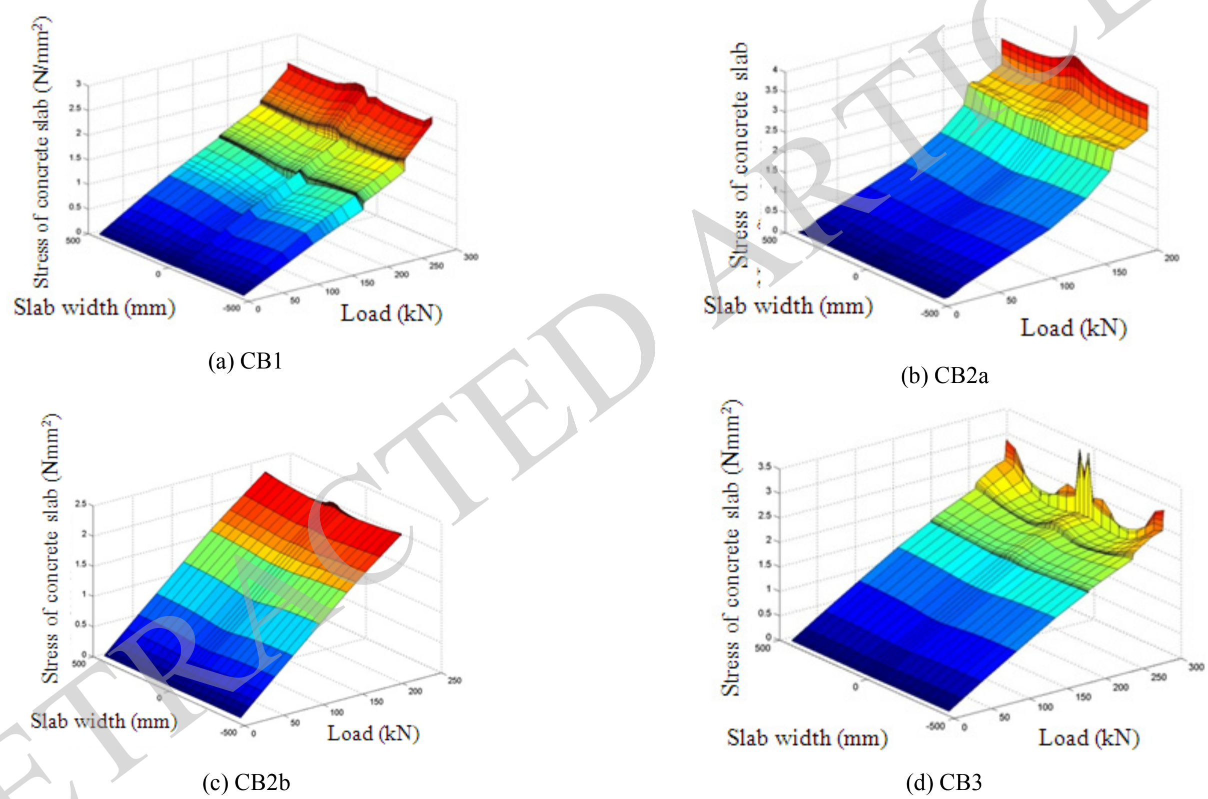

Fig. (18). Distribution of stress along the plate width direction.

numerical results. Therefore, shear lag should be paid great attention when designing and calculating the bearing capacity and deformation of SCCTG.

CONCLUSION

This article presents an overview of the test program in which four full-scale steel-concrete composite truss girder specimens are included. Specimens are loaded to failure to examine the the bending capacity of SCCTG. In this research, stress distribution, load-displacement relationship, load-slip relationship and ultimate bending capacity of SCCTGs are investigated. Major conclusions in this study are as follows:

(1) The damage evolution of SCCTG under bending load includes bottom slab crack at concrete slab, bottom chord member yielding, vertical crack fissures growing and penetrating along the slab, bottom chord full-section yield and compressive slab region crush.

(2) The whole section of SCCTG follows the plane section assumption generally.

(3) Bottom chord and shear connecting degree produce great influences on beam performances. SCCTGs with high shear connecting degree display fine bending and ductile behavior.

(4) Three-dimensional numerical model by finite element package ABAQUS is established to examine the bending

behaviour of SCCTG. An acceptable correlation has been observed between the analytical and experimental results. There is obvious shear lag effect in the concrete compression flange. Shear lag should be paid great attention when designing SCCTG.

CONFLICT OF INTEREST

The authors confirm that this article content has no conflict of interest.

ACKNOWLEDGEMENTS

The presented work was supported by Zhejiang Provincial Natural Science Foundation of China through Grant No. Y1100387 and by Vocational College Professional Leading Project of Zhejiang Province through Grant No. lj2013143. Sincere thanks are extended to School of Civil Engineering, Zhengzhou University for continuous support on the experiments.

REFERENCES

[1] D. Samuelson, "Composite Steel Joists," *Engineering Journal*, no. 3, pp. 111-120, 2002.

[2] Y. Wang, and T. Li, "Research summary on steel-concrete composite truss girder," *Steel Construction*, vol. 27, no. 2, pp. 1-5, 2012.

[3] B. F. Woldegiorgis, and D.J.U L. Kennedy, "Some behavioral aspects of composite trusses", *Structural Engineering Report,* no. *195,* University of Alberta, 1994.

[4] D. Samuelson, "Ite Joist Advantage", *Odern Steel Construction*, 2003.

[5] Y. Wang, T. Li, and R. Dong, "Performance Analysis of Steel-concrete Composite Truss Girder", *Chitecture Technology*, vol. 4, no. 3, pp. 216-218, 2013.

[6] Y. Wang, and T. Li, "Research of Ductile Ability on Composite Beam", *World Earthquake Engineering*, vol. 29, no. 1, pp. 102-107, 2013.

[7] J.R.U. Mujagic, W.S. Easterling, and T.M. Murray, "Design and behavior of light composite steel-concrete trusses with drilled standoff screw shear connections", *Journal of Constructional Steel*, vol. 66, no. 12, pp. 1483-1491, 2010.

[8] "The ASCE Task Committee on Design Criteria for Composite Structures in Steel and Concrete, Proposed specification and commentary for composite joists and composite trusses*," Journal of Structural Engineering*, pp. 350-358, 1996.

[9] R. P. Johnson, "Composite structures of steel and concrete", *Beams, Columns, Frames and Applications in Building*, 2nd Ed. Oxford: Blackwell Scientific, 1994.

[10] D. A. Nethercot, "Composite Construction," *New York: Taylor and Francis*, 2003.

Received: February 03, 2015 Revised: April 03, 2015 Accepted: May 25, 2015